Appl. Phys. A 72, 629–632 (2001) / Digital Object Identifier (DOI) 10.1007/s003390100796

Applied Physics A
Materials
Science & Processing

Rapid communication

Synthesis and Raman scattering of GaN nanorings, nanoribbons and nanowires

Z.J. Li[1,2], X.L. Chen[1,*], H.J. Li[2], Q.Y. Tu[1], Z. Yang[1], Y.P. Xu[1], B.Q. Hu[1]

[1] Institute of Physics and Center for Condensed Matter Physics, Chinese Academy of Sciences, Beijing 100080, P.R. China
[2] College of Materials Science and Engineering, Northwestern Polytechnical University, Xian 710072, P.R. China

Received: 16 November 2000/Accepted: 17 November 2000/Published online: 21 March 2001 –

Abstract. Low-dimensional GaN materials, including nanorings, nanoribbons and smooth nanowires have been synthesized by reacting gallium and ammonia using Ag particles as a catalyst on the substrate of MgO single crystals. They were characterized by field emission scanning electron microscopy (FE-SEM), energy dispersive X-ray spectroscopy (EDX) and X-ray diffraction (XRD). EDX, XRD indicated that the low-dimensional nanomaterials were wurtzite GaN. New features are found in Raman scatterings for these low-dimensional GaN materials, which are different from the previous observations of GaN materials.

PACS: 81.05.Ea; 42.65.Dr

GaN, a wide, direct band gap semiconductor (3.4 eV at room temperature), is an ideal material for the fabrication of blue and ultraviolet light-emitting diodes and high-temperature/high-power electronic devices [1–4]. Gallium nitride with low-dimensional structure is known to have great potential to address fundamental issues about dimensionality and to play a key role in novel nano-technological applications [4–9]. Much effort has been made in synthesizing GaN nanowires or nanorods. Recently, twisted and curved GaN nanowires or nanorods have been produced by chemical reactions in confined spaces provided by carbon nanotubes [10], GaAs nano-columns [11], and nanosized-pore Al_2O_3 templates [12]. The size and morphology of grown nanowires, however, rely on the templates to a large extent using this method. More recently, straight and smooth GaN nanowires have been fabricated on substrates by using catalysts [13]. The vapor–liquid–solid (VLS) growth mechanism is thought to be involved in the latter method. The main feature of the VLS crystal growth mechanism is the presence of intermediates that serve as catalysts between the vapor feed and the solid growth at elevated temperatures under chemical-vapor-deposition conditions. Gold and 3*d*-transition metals have been commonly used as catalysts for the synthesis of one-dimensional nanomaterials. In our work we found that the element silver is an ideal catalyst in the reaction of gallium and ammonia to form GaN nanowires on the substrate of MgO (100). Moreover, we found that nanorings and nanoribbons can be formed under certain conditions. Although the detailed mechanism in the ternary phase diagrams of Ag-Ga-N is still not fully understood, we suggest that very small miscible droplets of Ag-Ga-N may be generated rapidly during the heating process of the reaction and hence act as nucleation sites in the VLS growth of GaN nanomaterials. In this letter, we report the observations of new GaN low-dimensional nanomaterials and some new features in Raman scattering for these nanomaterials.

In a typical run, cubic magnesium oxide crystal substrates were quickly dipped in $AgNO_3$–ethanol solution (concentration 0.005–0.01 M). After being dried in air, the substrates were transferred into a horizontal quartz tube placed in a furnace, and heated at 450–550 °C in a stream of Ar for 20–30 min. The scanning electron microscopy (SEM) images indicated that Ag particles of about 8–15 nm (Fig. 1a) and 50–80 nm (Fig. 1b) in size formed on the surfaces of the substrates under different preparation conditions. The substrates distributed by Ag nanoparticles and Ga metals, were separated by a desired distance in a quartz boat and loaded into a long quartz tube under an Ar atmosphere. A desired steady NH_3 flow was started and maintained for different times at certain temperatures. Then the quartz tube was quickly cooled down with the NH_3 flow turned off. A light yellow layer was found on the substrates. The reaction used to synthesize GaN low-dimensional nanomaterials can be expressed as $Ga + NH_3 \rightarrow GaN + H_2$. However, GaN nanomaterials of different morphologies can be obtained by changing the size of the Ag particles, the flow of the ammonia, the duration, the distance between the substrates and the Ga etc.

The morphology and composition of the products were characterized using a Hitachi (Tokyo, Japan) S-4200 field emission scanning electron microscope (FE-SEM) equipped with energy dispersive X-ray (EDX) spectroscopy. The FE-SEM images (Figs. 2–4) show the different morphologies of the GaN nanomaterials. It is found that the nanorings are dominant under the conditions of relatively low temperature and flow of ammonia. The typical preparation con-

*Corresponding author. (E-mail: xlchen@aphy.iphy.ac.cn)

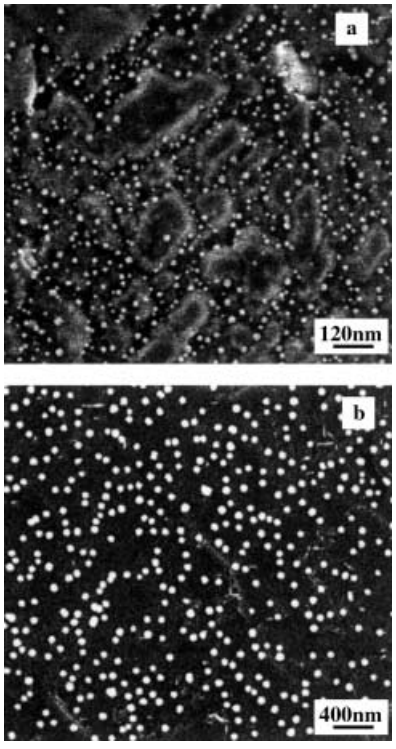

Fig. 1a,b. FE-SEM images of Ag nanoparticles of about **a** 8–15 nm or **b** 50–80 nm in size formed on the substrate of MgO (100) single crystals

ditions were as follows: The heating-up temperature was 930–950 °C, the flow of ammonia was about 13 cm^3/min and was maintained for 10–20 min and the distance between the substrate and the Ga was about 15–20 mm. The FE-SEM images of the GaN nanorings (Fig. 2) show that the width was about 100 nm (Fig. 2a,b) and 200 nm (Fig. 2c,d), the thickness was about 3–5 nm (Fig. 2a,b) and 5–10 nm (Fig. 2c,d) and the diameter was about 1.5–3 μm. However, under the conditions of relatively high temperature and flow of ammonia the nanoribbons were dominant. Figure 3 shows the FE-SEM images of the GaN nanoribbons (a NH_3 flow of about 15 cm^3/min was started and maintained for 10–20 min at 950–960 °C and the distance between the substrate and the Ga was 15–20 mm), which shows that the widths of the GaN nanoribbons were about 100–130 nm (Fig. 3a) and 50–70 nm (Fig. 3b) and the thicknesses of the GaN nanoribbons were about 3–10 nm. At further low temperatures and low flows of ammonia nanowires were formed. Figure 4 shows the FE-SEM images of GaN nanowires (a NH_3 flow of about 10 cm^3/min was started and maintained for 5–10 min at 870–890 °C and the distance between the substrate and the Ga was 20–25 mm) which shows that the GaN nanowires had diameters of 10–20 nm (Fig. 4a) and 40–70 nm (Fig. 4b) and a maximum length of about 500 μm (the result of the electrostatic charging is indicated by the arrows since the MgO substrate is an insulator). Figures 2–4 show also that we can obtain different sizes of GaN nanomaterials by changing the preparation parameters. The EDX analysis indicates that all GaN low-dimensional nanomaterials have the same composition of gallium and nitride with an atomic ratio of about 1 : 1, corresponding to the stoichiometric composition of GaN.

We found that the formation of GaN nanomaterials of different morphologies is dependent on the size of the Ag

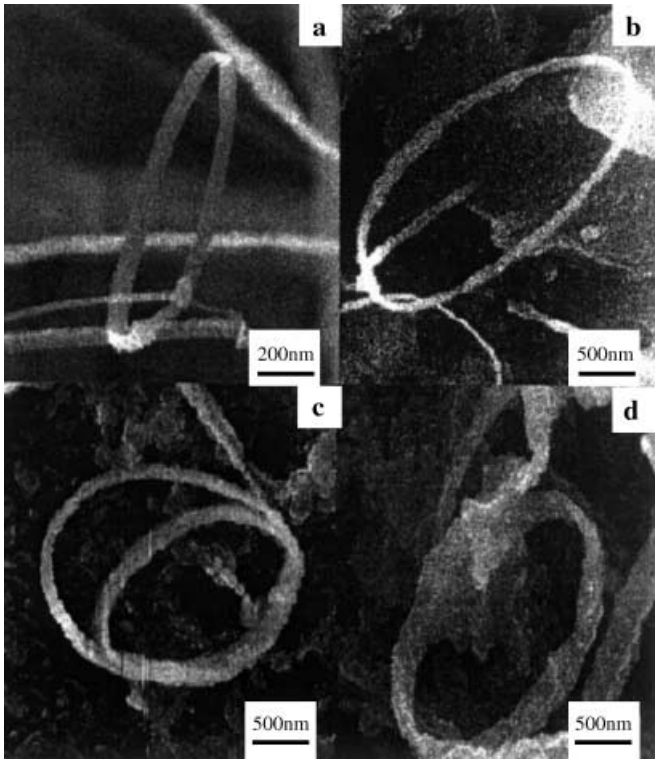

Fig. 2a–d. FE-SEM images of GaN nanorings with diameters of about 1.5–3 μm. **a**,**b** The width of the GaN nanorings is about 100 nm and the thickness is about 3–5 nm; **c**,**d** the width of the GaN nanorings is about 200 nm and the thickness is about 5–10 nm

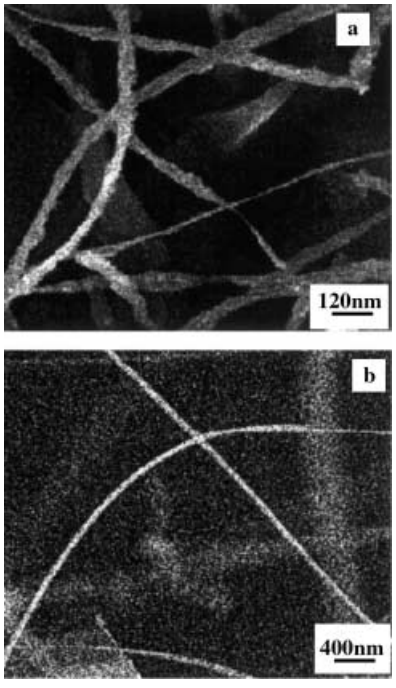

Fig. 3a,b. FE-SEM images of GaN nanoribbons; the width of the GaN nanoribbons is about **a** 100–130 nm or **b** 50–70 nm, and the thickness of the GaN nanoribbons is about 3–10 nm

nanoparticles distributed on the substrates in addition to preparation parameters. The nanorings and nanoribbons grew on the substrates separated by about 50–80 nm Ag nanoparti-

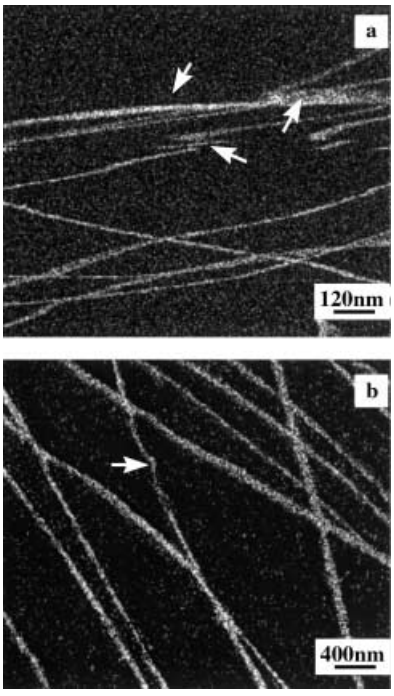

Fig. 4a,b. FE-SEM images of GaN nanowires; the GaN nanowires have diameters of about **a** 10–20 nm or **b** 40–70 nm (the result of the electrostatic charging is indicated by the arrows since the MgO substrate is an insulator)

cles but the growth of the nanowires required 8–15 nm Ag nanoparticles distributed evenly on the substrates. It is known that the melting point of the nanoparticles is much lower than that of the bulk material and the smaller the size, the lower the melting point. Only at higher temperatures can 50–80 nm Ag nanoparticles be melted, and they served as the liquid in the growth using the VLS mechanism. The higher temperature promoted Ag droplets and dissolved more gallium and nitrogen atoms, making the liquid drops bigger. Bigger droplets made GaN nanowires with bigger diameters than those grown using the VLS mechanism, so that they needed more time. The rates of growth were different in the different orientations due to the layer nature of the wurtzite structure GaN. The rate of growth in the [010] orientation was faster compared with those in the vertical directions. We assumed that the fiber direction of the nanowire was along one direction, say [120] [13]. Then [010] was perpendicular to the fiber. This led to a case where one radial direction [010] perpendicular to the fiber was the fast growth direction, and the other direction perpendicular to the fiber, e.g. [001], was a slow one. If a nanowire was very thin, the duration of growth was short. The difference in crystal growth in the two radial orientations was not obvious. But if the nanowire was wide, the duration of the growth was long. The growth difference in the two radial orientations became distinct. As a result the nanoribbon formed, in which [010] was across the width direction and [001] was along the thickness direction. On the other hand, if [010] was along the fiber direction, it was not possible to form the nanoribbon. The possible cause for the formation of the nanorings is as follows. At the lower temperature, the growth rate of the nanoribbons is slow. In the initial stages of nanoribbon growth, nanoribbons are bent by the gas flow. When ends of the nanoribbons contacted each other somewhere they easily tied together owing to the greater number of structure defects at the ends of the nanoribbons. Nanorings were formed in this way; the tail on each nanoring confirmed this (Fig. 2). The VLS growth mechanism of nanowires has been reported [14]. To test the role of the catalyst Ag nanoparticles, we repeated the experiment using a bare MgO crystal substrate under the same preparation conditions, and found that neither GaN nanoribbons and nanorings nor smooth nanowires formed.

To identify the overall crystal structure of the GaN nanomaterials of different morphology, all nanomaterials were characterized using a Rigaku (Tokyo, Japan) D/max-2400 X-ray diffractometer with Cu K_α radiation at room temperature. They all exhibited the same X-ray diffraction pattern. Figure 5 shows a typical X-ray diffraction spectrum which can indicate that the products are wurtzite GaN with lattice constants $a_0 = 3.18$ Å and $c_0 = 5.18$ Å. These values are in good agreement with the previously reported values [14]. Note that all reflections are broadened due to the size effect. The reflection peak at $2\theta = 42.92°$ corresponds to the (200) reflection of the cubic magnesium oxide crystal substrate.

We carried out studies of the Raman scattering of the GaN nanomaterials. The Raman backscattering measurements were performed at room temperature using a Spex 1403 Raman scattering spectrometer and an Ar^+ laser with 488 nm incident wavelength and 200 mW output power as the excitation source. Similar results were obtained in all GaN nanomaterials of different morphologies (Fig. 6). Figure 6(a)–(d) correspond to the nanoribbons, nanorings, smooth nanowires and MgO single crystal substrate, respectively. Figure 6 shows that no Raman mode is observed from a bare MgO crystal substrate (Fig. 6(d)), and only two strong peaks at about 560–569 cm^{-1} and 717–723 cm^{-1} are observed, corresponding in energy to the E_2 (high) and A_1 (LO) modes, respectively. They have some similar new features that are different to the previous observations of the GaN crystal [16, 17]. First, the peaks are obviously broad and asymmetrical for all samples and these phenomena become distinct as the morphology charges from nanoribbons to nanowires. Second, $I_{E_2}/I_{A_1(LO)} \leq 1$, which is contrary to the

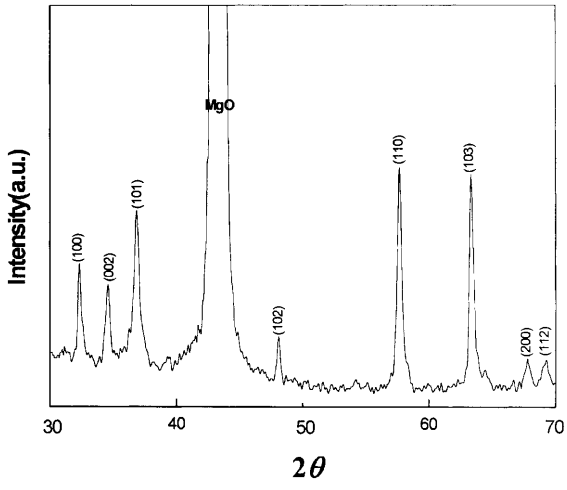

Fig. 5. XRD pattern obtained from a typical GaN nanomaterial. The reflection peak at $2\theta = 42.92°$ corresponds to the (200) reflection of the cubic magnesium oxide crystal substrate

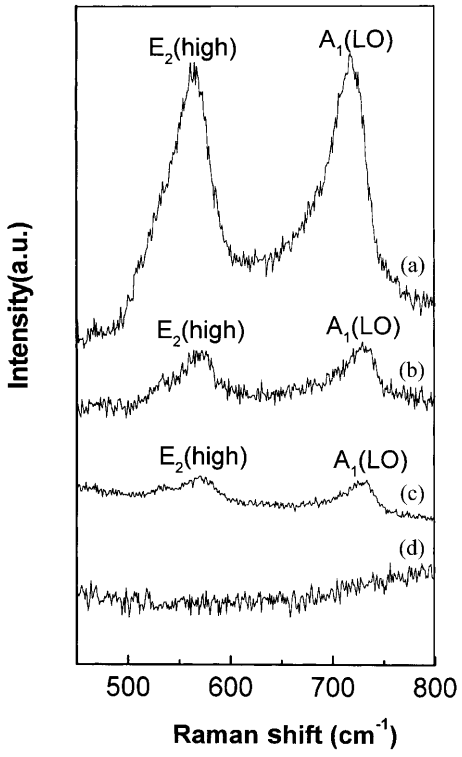

Fig. 6. Raman backscattering spectra of the GaN nanomaterials of different morphologies and the MgO single crystal substrate, (a), (b), (c), and (d) correspond to the nanoribbons, nanorings, smooth nanowires and MgO single crystal substrate, respectively

usually observed result of a high intensity ratio of $I_{E_2}/I_{A_1(LO)}$. Third, the A_1(LO) phonon frequency at 717–723 cm^{-1} shows a low-energy shift of 7–13 cm^{-1} compared to the previously reported values [16, 17]. The reasons for all the uniqueproperties may be due to the different morphologies of the GaN low-dimensional nanomaterials, the effect of the nanosize, the surface states and the existence of defects etc.

In conclusion, we have described an efficient approach for the synthesis of different morphologies of GaN low-dimensional nanomaterials (isolated nanorings, nanoribbons and smooth nanowires) by reacting gallium and ammonia using Ag particles as a catalyst on substrates of single crystal MgO. The results prove that we can obtain different morphologies and different sizes of GaN nanomaterials via rational selection of the catalyst, substrate and process parameters, and the results of the Raman scattering of the different morphologies of GaN nanomaterials also show some unique properties. All these results suggest possible applications in nanotechnology optoelectronic devices. Our experiments reveal that it will be straightforward to extend our method to fabricate the different morphologies of the nanomaterials of other nitrides and oxides.

Acknowledgements. This project was financially supported by the National Natural Science Foundation of China (NSFC) and the Chinese Academy of Science (CAS). Ms. C.Y. Wang, Mr. Y.L. Liu and Mr. T.S. Ning are acknowledged for their help in the work.

References

1. S. Nakamura: Science **281**, 956 (1998)
2. X.L. Chen, J.K. Liang, Y.P. Xu, T. Xu, P.Z. Jiang, Y.D. Yu, K.Q. Lu: Mod. Phys. Lett. B **13**, 285 (1999)
3. G. Fasol: Science **272**, 1751 (1996)
4. Q. Chen, M.A. Khan, J.W. Wang, C.J. Sun, M.S. Shur, H. Park: Appl. Phys. Lett. **69**, 794 (1996)
5. H. Morkoc, S.N. Mohammad: Science **276**, 51 (1995)
6. F.A. Ponce, D.P. Bour: Nature **386**, 351 (1997)
7. C.M. Lieber: Solid State Commun. **107**, 607 (1998)
8. K. Hiruma, M. Yazawa, T. Katsuyama, K. Ogawa, K. Haraguchi, M. Koguchi, H. Kakibayashi: J. Appl. Phys. **77**, 44 (1995)
9. J.Y. Li, X.L. Chen, Z.Y. Qiao, Y.G. Cao, M. He, T. Xu: Appl. Phys. A **71**, 349 (2000)
10. W.Q. Han, S.S. Fan, Q. Li, Y. Hu: Science **277**, 1287 (1997)
11. A. Hashimoto, T. Motiduki, H. Wada, A. Yamamoto: Mater. Sci. Forum **264–268**, 1129 (1998)
12. G.S. Cheng, L.D. Zhang, Y. Zhu, G.T. Fei, L. Li, C.M. Mo, Y.Q. Mao: Appl. Phys. Lett. **75**, 2455 (1999)
13. X.L. Chen, J.Y. Li, Y.G. Cao, Y.C. Lan, H. Li, M. He, C.Y. Wang, Z. Zhang, Z.Y. Qiao: Adv. Mater. **12**, 1432 (2000)
14. C.C. Chen, C.C. Yeh: Adv. Mater. **12**, 738 (2000)
15. X.F. Duan, C.M. Lieber: J. Chem. Soc. **122**, 188 (2000)
16. G.H. Li, W. Zhang, H.X. Han, Z.P. Wang: J. Appl. Phy. **86**, 2051 (1999)
17. Y.G. Cao, X.L. Chen, Y.C. Lan, Y.P. Xu, T. Xu, J.K. Ling: J. Mater. Res. **15**, 267 (2000)